ON A CLASS OF TRANSFER FUNCTIONS SUITABLE FOR VIDEO NETWORKS

R. M. FANO

TECHNICAL REPORT NO. 155

APRIL 13, 1950

RESEARCH LABORATORY OF ELECTRONICS
MASSACHUSETTS INSTITUTE OF TECHNOLOGY

The research reported in this document was made possible through support extended the Massachusetts Institute of Technology, Research Laboratory of Electronics, jointly by the Army Signal Corps, the Navy Department (Office of Naval Research) and the Air Force (Air Materiel Command), under Signal Corps Contract No. W36-039-sc-32037, Project No. 102B; Department of the Army Project No. 3-99-10-022.

MASSACHUSETTS INSTITUTE OF TECHNOLOGY

RESEARCH LABORATORY OF ELECTRONICS

Technical Report No. 155

April 13, 1950

ON A CLASS OF TRANSFER FUNCTIONS SUITABLE FOR VIDEO NETWORKS

R. M. Fano

Abstract

This report deals with a new class of transfer functions suitable for video networks. The resulting unit-step response has a very small amount of overshoot which is almost independent of the algebraic degree of the corresponding transfer function. The applications of such functions to the design of video filters and amplifiers is discussed in some detail.

ON A CLASS OF TRANSFER FUNCTIONS SUITABLE FOR VIDEO NETWORKS

I. Introduction

The first step in the design of filters or amplifiers is the selection of an appropriate transfer function corresponding to a network of desired complexity. In the particular case of video networks, the unit-step response must have a specified rise time and must be free from appreciable overshoot. In addition, the network might be required to have a specified channel discrimination, or, in the case of an amplifier, might have to accommodate enough tubes to provide a prescribed gain. Both the rise time and the overshoot are controlled chiefly by the pass-band behavior of the transfer function. On the other hand, the network complexity, that is, the number of elements, depends primarily on the rejection-band characteristics. A type of transfer function commonly used in connection with video systems is that derived (1) from the Butterworth function

$$\frac{1}{\sqrt{1 + x^{2n}}} \tag{1}$$

which represents the absolute value at real frequencies. This type of function has the disadvantage that the overshoot increases with increasing n, exceeding 11 percent for $n > 4$ (2). Thus the channel discrimination and the number of tubes that can be accommodated are rather limited, if the overshoot is to be kept small. This unsatisfactory type of behavior arises from the fact that the pass-band characteristics and the network complexity (degree of the function) cannot be controlled independently.

The class of functions discussed in this report involves a parameter which can be adjusted for proper pass-band behavior. By using transfer functions of this type it is possible to keep the overshoot within satisfactory limits regardless of the network complexity. In addition the singularities are distributed over the complex plane in such an orderly manner that the synthesis problem and the derivation of important system characteristics are considerably simplified.

After a study of the functions themselves, the report will present some typical applications to the design of video filters and amplifiers.

II. A Class of Transfer Functions

The unit-step response of a linear network depends primarily, as pointed out above, on the pass-band behavior of the transfer function. More specifically, the rise time is inversely proportional to the bandwidth, and the general form of the time function, including the overshoot, depends on the shape of the amplitude and phase characteristics. It must be remembered in this connection that the phase characteristic is entirely specified by the amplitude in the case of minimum-phase networks. Although time-domain characteristics, such as the amount of overshoot, are not simply related to frequency-domain characteristics, it is possible to state, in an approximate fashion, which type of pass-band behavior leads to a unit-step response substantially free from overshoot.

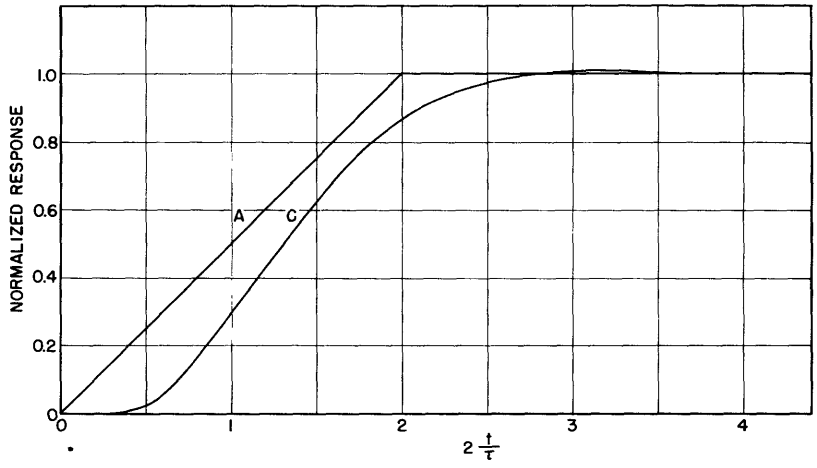

Fig. 1 Unit-step responses corresponding to the amplitude characteristics A and C of Fig. 2.

The most desirable type of unit-step response is that represented by curve A in Fig. 1. The minimum-phase transfer function yielding this response is found to be

$$t(x) = \frac{\sin x}{x} e^{jx} \qquad (2)$$

where x is the normalized frequency variable

$$x = \omega \frac{\tau}{2} \qquad (3)$$

and τ is the rise time. The absolute value (amplitude characteristic) of this function over the pass band is plotted on a decibel scale as curve A in Fig. 2. The phase characteristic is linear for all values of x.

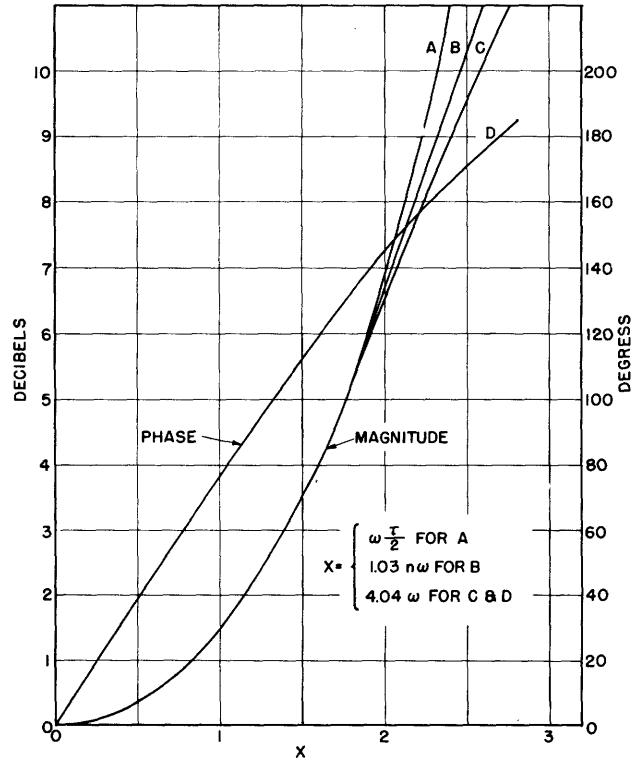

Fig. 2 Amplitude and phase characteristics.

Although the transfer function of Eq. 2 meets the conditions of physical realizability (3), it cannot be realized with a finite number of elements. E. A. Guillemin (3) has argued, however, that any transfer function which approximates Eq. 2 over the pass band should have a unit-step response reasonably close to the ideal response of Fig. 1. Such an argument has been rather successful in many practical cases. The effect of deviations from the ideal function of Eq. 2 may be easily estimated by following, for instance, the "paired-echoes" technique suggested by Wheeler (4).

The general considerations given above indicate that the unsatisfactory unit-step

response of the Butterworth function for large values of n, results from the fact that the amplitude response is too flat over the pass band. Oscillatory pass-band behavior as obtained by means of Tchebycheff polynomials (5, 6) would yield an even larger overshoot. It is important to note, in this regard, that the poles of the Butterworth transfer functions are uniformly distributed (1) over a semicircle centered at the origin and extending in the left half of the complex plane, as indicated in Fig. 3a. In the case of transfer

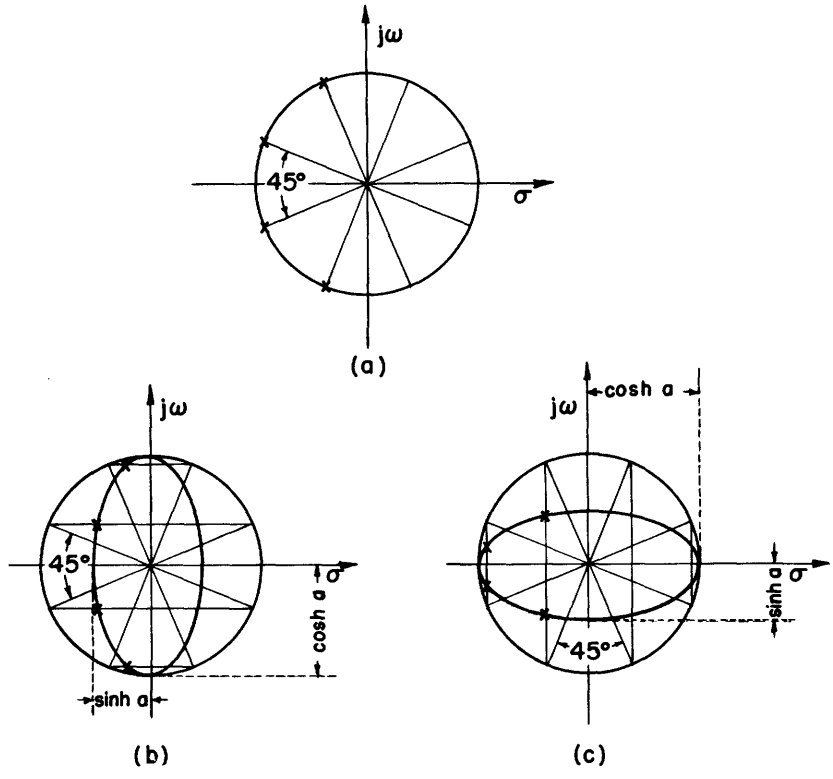

Fig. 3 Pole distributions of three types of transfer functions.

functions of the Tchebycheff type, the poles lie on the left half of an ellipse centered at the origin and with its major axis coinciding with the imaginary axis of the complex plane (see Fig. 3b). The ratio of the semi-axes may be expressed as the hyperbolic tangent of a parameter a. Thus the case of the Butterworth functions may be considered as the limiting case of the Tchebycheff functions for $a = \infty$. If we relate the characters of these pole distributions to the corresponding unit-step responses, it becomes clear that passing from the distribution of Fig. 3b to that of Fig. 3a is a step in the right direction when a small overshoot is desired. The next logical step is to turn the elliptical pole distribution 90° to make the minor axis coincide with the imaginary axis of the complex plane, as shown in Fig. 3c. The parameter a controlling the shape of the ellipse can still be adjusted to optimize the unit-step response, as shown below.

Following the same procedure as in the case of the Tchebycheff transfer functions (6), the magnitude squared of any transfer function $t(\lambda)$ having a pole distribution of the type illustrated in Fig. 3c is found to be

$$\left|t(\lambda)\right|^2_{\lambda=j\omega} = T(\omega) = \frac{A}{\sinh^2 na + \cosh^2(n \sinh^{-1}\omega)} \tag{4}$$

where A is an arbitrary constant. The location of the poles of $t(\lambda)$ is given by

$$\lambda_p = \cosh\left\{a + j\left[\frac{\pi}{2} + \frac{\pi}{n}(m + \frac{1}{2})\right]\right\} \tag{5}$$

for $m = 0, 1, 2, \ldots, n - 1$.

The optimum value of the parameter a may be obtained by comparing the log log plot of $T(\omega)$ with a similar plot of $\sin^2 x/x^2$. It turns out that for $n \geq 4$ the optimum value of a is given by

$$a = \frac{1.2}{n} \tag{6}$$

corresponding to $\sinh^2 na = 2.25$. The case of $n < 4$ has not been considered in detail because the unit-step behavior of low-pass networks with less than four elements has been investigated extensively by many authors. One may expect that the optimum value of a would be somewhat larger in these extreme cases.

The behavior of $T(\omega)$ for $n = 4$ and $A = 3.25$ is shown as curve C in Fig. 2. The corresponding phase characteristic is shown as curve D in the same figure. The 3-db points of A and C are made to coincide by normalizing the frequency scale. Curves A and C differ by less than 0.05 db over the attenuation range from 0 to 4 db. The phase characteristic D is linear within 1 degree over the corresponding frequency range and within 8 degrees over a frequency range equal to twice the pass band. The computed unit-step response for $n = 4$ is shown in Fig. 1 as curve C, in which the time scale is normalized to correspond to the frequency scale in Fig. 2. Thus curves A and C of Fig. 1 correspond to transfer functions with the same 3-db point. The overshoot is less than 1 percent, and the rise time between 0.025 and 0.975 is equal to 2, as for the ideal response represented by curve A.

Considering the case of $n > 4$, we observe that the pass band corresponds to values of ω so small that they do not differ appreciably from $\sinh^{-1}\omega$. This approximation which is certainly satisfactory for large values of n is reasonably good even for $n = 4$. In fact, for $n = 4$, the difference between ω and $\sinh^{-1}\omega$ at the 3-db point is still only 2 percent. It seems reasonable then to use such an approximation in determining the optimum value of a for $n > 4$. As a matter of fact the optimum value of $\sinh^2 na$ does not change appreciably from 2.25, the value that was found optimum for $n = 4$. Curve B in Fig. 2 illustrates the pass-band behavior of the function

$$\frac{3.25}{2.25 + \cosh^2 n\omega} \quad . \tag{7}$$

Curve B approaches the ideal behavior represented by curve A even better than curve C. Thus we may expect that for $n > 4$ the unit-step response will approach even closer the ideal time function of Fig. 1. However, because of the labor involved, no computation has been performed for $n > 4$. The frequency scale for curve B of Fig. 2 has been

normalized, as in the case of curve A to make the 3-db point coincide with that of curve A. More precisely, in this case

$$x = 1.03\, n\omega \quad . \tag{8}$$

Thus, the value of ω at the 3-db point is inversely proportional to n. On the other hand the optimum value of a is also inversely proportional to n as indicated by Eq. 6. Thus if the frequency scale of $t(\lambda)$ is readjusted to keep the bandwidth constant when n is increased, the minor semi-axis of the ellipse on which the poles lie remains practically unchanged. In fact, if the value of x at the 3-db point is kept fixed at 1.39 as in Fig. 2,

$$\text{minor semi-axis} = n \sinh \frac{1.2}{n} \quad . \tag{9}$$

The major semi-axis, on the contrary, becomes proportional to n for large values of n, if the 3-db point is kept constant. In fact

$$\text{major semi-axis} = n \cosh \frac{1.2}{n} \quad . \tag{10}$$

A last important characteristic of $T(\omega)$ is the behavior for large values of ω. For such values of ω, $\ln 2\omega$ may be substituted for $\sinh^{-1}\omega$ and an exponential for the hyperbolic cosine, so that

$$T(\omega) \approx \frac{3.25}{2.25 + \left[\frac{1}{2}(2\omega)^n\right]^2} \quad . \tag{11}$$

In conclusion $T(\omega)$ approaches zero as ω^{-2n}, or the attenuation for large values of ω increases at the rate of 6n db per octave.

III. Filter Applications

The function $T(\omega)$ of Eq. 4 may be used as the magnitude squared of the transmission coefficient of a lossless filter, that is as the ratio of the load power to the power available from the source. In this case the arbitrary constant A must be smaller than or equal to $\cosh^2 na$, because the power ratio represented by $T(\omega)$ cannot be larger than one. Since all the zeros of $T(\omega)$ are located at infinity, the filter may be synthesized in the form of a ladder structure of inductances and capacitances with a total number of elements equal to n.

The determination of the element values may be performed in a number of ways, a discussion of which is beyond the scope of this report. On the other hand, the type of functions discussed above falls within the range of a particularly convenient procedure developed by the author in connection with the design of broadbanding networks (7). This procedure leads very quickly to the element values as soon as certain parameters, functions of a and n, are known. It seems worthwhile, therefore, to derive expressions for these parameters (equal in number to the elements of the filter) and to discuss a few additional details of the procedure. The values of the n parameters in question, using the terminology of Ref. 7, are given by

$$A^{\infty}_{2k+1} = \frac{1}{2k+1}\left[\sum_i \lambda_{oi}^{2k+1} - \sum_i \lambda_{pi}^{2k+1}\right] \qquad \text{for } k = 0, 1, \ldots, n-1 \qquad (12)$$

where the λ_{pi} and the λ_{oi} are, respectively, the poles and the zeros of either reflection coefficient of the filter. The magnitude squared of the reflection coefficient is related to $T(\omega)$ of Eq. 4 by

$$\left|\rho_1(\lambda)\right|^2_{\lambda=j\omega} = \left[\rho_1(\lambda)\,\rho_1(-\lambda)\right]_{\lambda=j\omega} = 1 - T(\omega) = \frac{(\sinh^2 na - A) + \cosh^2(n \sinh^{-1}\omega)}{\sinh^2 na + \cosh^2(n \sinh^{-1}\omega)}. \qquad (13)$$

The poles and the zeros of this function form arrays symmetrical with respect to the imaginary axis of the λ-plane. The poles of $\rho_1(\lambda)$ must be those poles of the function $\rho_1(\lambda)\,\rho_1(-\lambda)$ which lie in the left half-plane, if $\rho_1(\lambda)$ is to be physically realizable. The zeros of $\rho_1(\lambda)$, however, may lie in either half of the complex plane; the only restriction is that they must be selected in conjugate pairs from each quadruplet of symmetrical zeros of the function of Eq. 13. The reflection coefficient $\rho_2(\lambda)$ measured at the opposite end of the filter (8) has the same poles as $\rho_1(\lambda)$ but zeros symmetrically located with respect to the imaginary axis. Thus $\rho_1(\lambda)$ and $\rho_2(\lambda)$ share all the zeros of the function of Eq. 13. In the case of minimum phase networks and apart from a difference in sign, $\rho_2(\lambda)$ is completely specified by $\rho_1(\lambda)$. They have the same sign if the number n of elements is odd, and opposite signs if n is even (8).

It is clear that the poles of $\rho_1(\lambda)$ and $\rho_2(\lambda)$ are the same as the poles of $t(\lambda)$ as given by Eq. 5. If $\sinh^2 na > A$, the zeros of the function of Eq. 13 are similarly located on an ellipse specified by a parameter b which may be obtained from

$$\sinh^2 nb = \sinh^2 na - A \quad . \qquad (14)$$

Thus the location of the zeros is given by Eq. 5 in which b is substituted for a, and m takes all the values from 0 to 2n - 1. If $\sinh^2 na \leqslant A \leqslant \cosh^2 na$, the ellipse degenerates into a segment of the real axis and the zeros are given by

$$\sigma_o = \sin\frac{\pm\phi + 2m\pi}{n} \qquad m = 0, 1, \ldots, n-1 \qquad (15)$$

where $\phi = \cos^{-1}\sqrt{A - \sinh^2 na}$. In the particular case of a match at zero frequency ($T(0) = 1$, $A = \cosh^2 na$) Eq. 15 becomes

$$\sigma_o = \sin\frac{m\pi}{n} \qquad m = 0, 1, \ldots, 2n-1 \quad . \qquad (16)$$

The summations appearing in Eq. 12 can now be computed. We obtain for the poles

$$\left.\begin{aligned}
\sum_i \lambda_{\rho i} &= -\frac{\cosh a}{\sin \frac{\pi}{2n}} \\
\sum_i \lambda_{\rho i}^3 &= \frac{3}{4}\left[\frac{\cosh 3a}{3 \sin \frac{3\pi}{2n}} - \frac{\cosh a}{\sin \frac{\pi}{2n}}\right] \\
\sum_i \lambda_{\rho i}^5 &= -\frac{5}{16}\left[\frac{\cosh 5a}{5 \sin \frac{5\pi}{2n}} - \frac{\cosh 3a}{\sin \frac{3\pi}{2n}} + 2\frac{\cosh a}{\sin \frac{\pi}{2n}}\right] \\
\sum_i \lambda_{\rho i}^7 &= \frac{7}{64}\left[\frac{\cosh 7a}{7 \sin \frac{7\pi}{2n}} - \frac{\cosh 5a}{\sin \frac{5\pi}{2n}} + 3\frac{\cosh 3a}{\sin \frac{3\pi}{2n}} - 5\frac{\cosh a}{\sin \frac{\pi}{2n}}\right]
\end{aligned}\right\} . \qquad (17)$$

If $\sinh^2 na > A$ and the zeros of ρ_1 are selected in the left half-plane, the summations for the zeros of ρ_1 are given by Eq. 17 with b substituted for a. The summations for the zeros of ρ_2 are the negative of the corresponding expressions for ρ_1. If $\sinh^2 na < A$ the computations become so simple that the derivation of general formulas such as Eqs. 17 is unnecessary. In the special case of $A = \cosh^2 na$, the zeros of ρ_1 may be selected in such a symmetrical way that all summations become equal to ± 1 if n is even, and to zero if n is odd.

The computation of the element values follows as indicated in Ref. 7. The pertinent formulas are repeated below for the convenience of the reader.

$$a_1 = A_1^\infty \qquad a_3 = 4\frac{A_3^\infty}{(A_1^\infty)^3} - \frac{1}{3} \qquad a_5 = 16\frac{A_5^\infty}{(A_1^\infty)^5} - \frac{1}{5} \qquad a_7 = 64\frac{A_7^\infty}{(A_1^\infty)^7} - \frac{1}{7} \qquad (18)$$

$$\left.\begin{aligned}
L_1 &= \frac{2}{a_1} \qquad C_2 = -\frac{L_1}{a_3} \qquad L_3 = -\frac{a_3 L_1}{1 + a_3 - (a_5/a_3)} \\
C_4 &= \frac{\left[1 + a_3 - (a_5/a_3)\right]^2 L_1}{a_3\left[1 + a_3 - (a_5/a_3) + (a_5/a_3)^2 - (a_7/a_3)\right]}
\end{aligned}\right\} . \qquad (19)$$

The element values above correspond to a unit-resistance termination. The dual network with L and C interchanged is an alternative solution to the synthesis problem corresponding to the case in which the reflection coefficient is negative for large values of λ. Formulas for the fifth and following elements are not available. However, the case of an eight-element filter can still be handled by computing four elements from each end of the network. In this case, proper attention must be paid to the magnitude of the reflection coefficient at the origin, in order to determine the relative magnitudes of the terminating

resistances and, hence, of the inductive and capacitive elements.

The filter shown in Fig. 4 has been computed following the above procedure. The magnitude and phase of its transmission coefficient, $t(\lambda) = 2E_2/E_1$, are plotted in Fig. 2 as curves C and D; its unit-step response is represented by curve C of Fig. 1.

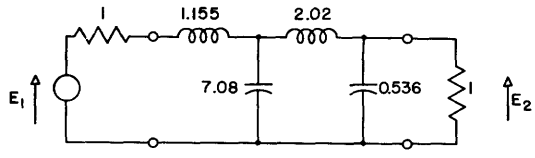

Fig. 4 Four-element low-pass filter; element values in ohms, henries and farads; 3-db point for $\omega = 0.344$.

The design procedure discussed above may also be used in connection with nondissipative networks open-circuited on one side. In this case the magnitude squared of the transmission coefficient vanishes over the whole imaginary axis since it represents the ratio of the load power to the power available from the source. The ratio of the output voltage E_2 to the source voltage E_1 remains finite. In fact for finite source and load resistances R_1 and R_2

$$\left|\frac{E_2}{E_1}\right|^2 = 4\,T(\omega)\,\frac{R_2}{R_1} \quad . \tag{20}$$

In other words the constant A of Eq. 4 approaches zero as $1/R_2$ when R_2 approaches infinity. In this case the reflection coefficient from the source side, ρ_1, has a magnitude equal to one over the whole imaginary axis but not over the rest of the complex plane. Consequently its zeros are located in the right half-plane at positions symmetrical to those of the poles. The reflection coefficient ρ_2 at the open-circuited terminals is equal to one over the whole complex plane because its zeros coincide with the poles. However, it is still possible to carry out the design procedure discussed above from the ρ_2 side through an appropriate limiting process. When R_2 approaches infinity, the parameter b (on which the locations of the zeros of ρ_2 depend) approaches a (the corresponding parameter for the poles). Thus the quantities A^{∞}_{2n+1} and α_{2n+1} may be expressed as differentials with respect to a($da = b - a$), while R_2 itself may be expressed as

$$\frac{1}{R_2} = -\frac{\tanh a}{8\,R_1}\,da \quad . \tag{21}$$

The net result is that R_2L_1, C_2/R_2, etc. remain finite when R_2 approaches infinity.

These design considerations were limited for convenience to the case of low-pass filters. However high-pass, band-pass, and band-elimination filters may be obtained from prototype low-pass filters by means of well-known transformations.

IV. Amplifier Applications

The function $T(\omega)$ of Eq. 4 may also be used to represent the magnitude squared of the transfer functions of an amplifier. In this case, again, the poles of $t(\lambda)$ must not lie in the right half-plane and must be selected in conjugate pairs from each set of poles of $T(\omega)$ symmetrically located with respect to the origin. In theory the constant of

proportionality A make take any real value, but in practice it is limited by the transconductance and interelectrode capacitances of the tubes available. Before discussing this very important limitation, it is necessary to consider how the amplifier coupling networks may be designed.

Let us consider first the case of low-pass (video) amplifiers. The transfer function of the whole amplifier is equal to the product of the transfer functions of the individual stages. Thus the poles of the overall function are shared by the stages in an arbitrary manner consistent with the physical realizability of the individual stages. The transfer function of any one stage may have the form of a self or of a transfer impedance depending on whether the interstage network is of the one-terminal-pair or two-terminal-pair type. In both cases the interstage network must include shunt capacitances across both the input and output terminals in order to absorb the interelectrode capacitances of the tubes.

In the case of a one-terminal-pair coupling network, the transfer function of the stage is given by the transconductance g_m of the tube (with a negative sign) multiplied by the impedance of the network. It follows that the transfer function may have only a simple zero at infinity. On the other hand $t(\lambda)$ has all its zeros at infinity. It follows that all finite zeros of one stage must be eliminated by coincident poles of other stages. A simple pair of stages whose transfer function has a pair of conjugate poles and a double zero at infinity is shown in Fig. 5. The transfer function of the first stage of the pair is

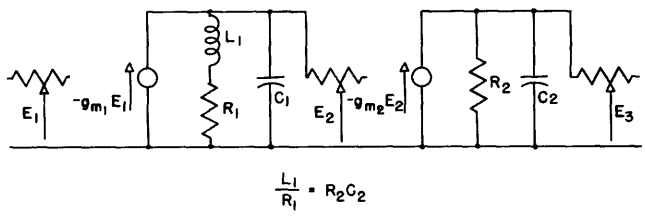

Fig. 5 A pair of amplifier stages.

$$\frac{E_2}{E_1} = -g_{m1}\frac{R_1 + L_1\lambda_1}{1 + R_1C_1\lambda + L_1C_1\lambda^2} \tag{22}$$

and that of the second stage is

$$\frac{E_3}{E_2} = -g_{m2}\frac{R_2}{1 + R_2C_2\lambda} \tag{23}$$

If we make

$$\frac{L_1}{R_1} = R_2C_2 \tag{24}$$

the transfer function of the pair becomes

$$\frac{E_3}{E_1} = g_{m1}g_{m2}\frac{R_1R_2}{1 + R_1C_1 + L_1C_1\lambda^2} = \frac{g_{m1}g_{m2}}{C_1C_2}\frac{1}{(\lambda - \lambda_o)(\lambda - \overline{\lambda}_o)} \tag{25}$$

where

$$\lambda_o = -\frac{R_1}{2L_1} + j\sqrt{\frac{1}{L_1C_1} - \left(\frac{R_1}{2L}\right)^2} \tag{26}$$

and $\bar{\lambda}_o$ form a pair of conjugate poles. The gain of the pair at zero frequency is

$$\left(\frac{E_3}{E_1}\right)_{\lambda=0} = \frac{g_{m1}\, g_{m2}}{C_1C_2\,|\lambda_o|^2} \tag{27}$$

where

$$|\lambda_o|^2 = \frac{1}{L_1C_1} \quad . \tag{28}$$

For identical tubes

$$\left(\frac{E_3}{E_1}\right)_{\lambda=0} = \frac{g_m^2}{C^2|\lambda_o|^2} \quad . \tag{29}$$

Fig. 6 illustrates a two-terminal-pair interstage network with the same poles and

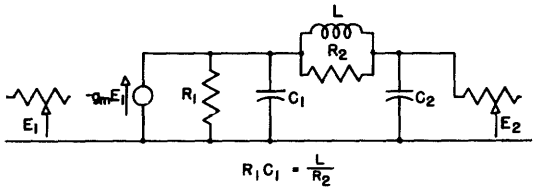

Fig. 6 An amplifier stage.

zeros as those of the two stages of Fig. 5. Its transfer function is

$$\frac{E_2}{E_1} = -g_m \frac{R_1}{R_1C_2\lambda + (1 + R_1C_1\lambda)\dfrac{R_2 + L\lambda + R_2LC_2\lambda^2}{R_2 + L\lambda}} \tag{30}$$

which, for

$$R_1C_1 = \frac{L}{R_2} \tag{31}$$

reduces to

$$\frac{E_2}{E_1} = -g_m \frac{R_1}{1 + \left(\dfrac{L}{R_2} + R_1C_2\right)\lambda + LC_2\lambda^2} = -\frac{2g_m\,\sigma_o}{C_1 + C_2}\,\frac{1}{(\lambda - \lambda_o)(\lambda - \bar{\lambda}_o)} \tag{32}$$

where

$$\lambda_o = \sigma_o + j\omega_o = \frac{R_1}{L}\,\frac{C_1 + C_2}{2C_2} + j\sqrt{\frac{1}{LC_2} - \left(\frac{R_1}{L}\,\frac{C_1 + C_2}{2C_2}\right)^2} \quad . \tag{33}$$

The gain of the stage at zero frequency is

$$\left(\frac{E_2}{E_1}\right)_{\lambda=0} = -\frac{2g_m \sigma_o}{(C_1 + C_2)|\lambda_o|^2} \quad . \tag{34}$$

A pole on the real axis may be obtained by means of a simple RC network, as in the second stage of Fig. 5, for which the zero-frequency gain is

$$\frac{E_2}{E_1} = -\frac{g_m}{C|\lambda_o|} \tag{35}$$

where

$$\lambda_o = -\frac{1}{RC} \quad . \tag{36}$$

If the transfer function $t(\lambda)$ is synthesized by means of stage-pairs of the type shown in Fig. 5, the overall zero-frequency gain becomes, for identical tubes

$$G_n = \left(\frac{g_m}{C}\right)^n \prod_1^n \frac{1}{|\lambda_k|} \quad . \tag{37}$$

This equation together with Eqs. 4, 5, and 6 yields

$$G_n = \frac{1}{3.6}\left(\frac{2.7\, g_m}{n\omega_c C}\right)^n \tag{38}$$

where ω_c is the half-power frequency.

If stages similar to that of Fig. 6 were used, the overall gain would become, for n even

$$G'_n = \left(-\frac{2g_m}{C}\right)^{\frac{n}{2}} \prod_1^n \frac{|\sigma_k|^{\frac{1}{2}}}{|\lambda_k|} \quad . \tag{39}$$

and, for n odd

$$G'_n = \frac{1}{2}\left(-\frac{2g_m}{C}\right)^{\frac{n+1}{2}} \left[\prod_1^n \frac{|\sigma_k|^{\frac{1}{2}}}{|\lambda_k|}\right] \frac{1}{|\sigma_o|^{\frac{1}{2}}} \quad . \tag{40}$$

The capacitance $C = C_1 + C_2$ is the total stage capacitance of Eqs. 37 and 38; σ_o represents the pole on the real axis. Using Eqs. 4, 5 and 6 we obtain finally, for n even

$$G_n' = \frac{1}{2.55}\left(\frac{5.4\, g_m \cosh \frac{1.2}{n}}{n\omega_c C}\right)^{\frac{n}{2}} \tag{41}$$

and, for n odd

$$G_n' = \frac{1}{7.2 \cosh \frac{1.2}{n}}\left(\frac{5.4\, g_m \cosh \frac{1.2}{n}}{n\omega_c C}\right)^{\frac{n+1}{2}} . \tag{42}$$

Equation 42 would be slightly different if the pole on the real axis were incorporated in one of the coupling networks by eliminating R_2 instead of being obtained by means of a separate RC stage. However, the main implications of Eq. 42 would not change.

Equations 38 and 41 indicate that the gain does not increase indefinitely with the number of stages but has a maximum for some value of n. In the case of Eq. 38 a maximum gain

$$G_{max} = \frac{1}{3.6} e^{\frac{K}{e}} \tag{43}$$

is obtained for

$$n = \frac{K}{e} \tag{44}$$

where

$$K = \frac{2.7\, g_m}{\omega_c C} . \tag{45}$$

In the case of Eq. 41, if we disregard the small effect of cosh (1.2/n), we obtain

$$G_{max} \simeq \frac{1}{2.55} e^{\frac{K'}{2e}} \tag{46}$$

for

$$n \simeq \frac{K'}{e} \tag{47}$$

and

$$K' \simeq \frac{5.4\, g_m}{\omega_c C} . \tag{48}$$

Since $K' \simeq 2K$, the maximum gain that can be obtained with two-terminal-pair networks is approximately $\sqrt{2}$ times larger than with one-terminal-pair networks. The advantage of the two-terminal-pair networks results from the fact that the input and output capacitances of the tubes are not lumped together. This result is consistent with the limiting conditions studied by Bode (9).

The existence of an upper limit to the gain might be surprising in view of the fact that

in the case of amplifiers having a Tchebycheff or a Butterworth transfer function, the gain may increase indefinitely with the number of stages. The reason for the different behavior is that in the latter case we require only a specified bandwidth, while in our case we require as well a unit-step response without appreciable overshoot. In the Tchebycheff and Butterworth cases the poles are located within a distance from the origin equal to the cut-off frequency, regardless of the number of poles. In our case, on the contrary, the poles lie on an ellipse whose minor semi-axis is proportional to the cut-off frequency ω_c. The ratio of the two axes, on the other hand, increases indefinitely with the number n of poles as coth (1.2/n). It follows that, for a given ω_c the n^{th} root of the product of the distances from the origin to the poles increases indefinitely with n; more precisely, is proportional to n. Equations 37 and 39 (which apply whenever all the zeros of the transfer function are at infinity) show clearly the dependence of the gain on the distances $|\lambda_k|$ of the poles from the origin.

The existence of an upper limit for the gain when the bandwidth is specified has been observed previously in the case of cascades of identical stages or groups of stages (10). It appears that this limitation is not the result of the cascading of identical stages but is a direct consequence of the requirement of negligible overshoot. In fact, it can be shown with the help of potential analogies that, if the poles of a function are restricted to a finite region of the complex plane, either the magnitude of the function approaches a rectangular shape when the number of poles increases indefinitely, or otherwise the bandwidth must decrease indefinitely. In our case the bandwidth decreases as 1/n, while in the case of cascaded RC stages it decreases approximately at $1/\sqrt{n}$. This difference has to do with the shape of the amplitude characteristics and, therefore, with the shape of the unit-step response.

The case of band-pass amplifiers does not differ substantially from that of low-pass amplifiers discussed above. The actual expressions for the gain depend on the way in which the poles are realized in the interstage networks. In the particular case of single-tuned stages (staggered-tuned amplifiers) the gain is still given by Eq. 38 in which the bandwidth (in rad/sec) is substituted for ω_c.

References

1. G. E. Valley, Jr., H. Wallman: Vacuum Tube Amplifiers, Vol. 18, Sec. 4.6, Radiation Laboratory Series (McGraw-Hill, N.Y. 1948).
2. G. E. Valley, Jr., H. Wallman: Loc. cit., Sec. 7.5.
3. G. E. Valley, Jr., H. Wallman: Loc. cit., Appendix A.
4. H. A. Wheeler: Proc. I.R.E. 27, 359 (1939).
5. S. Darlington: Jour. Math. Phys. 18, 275-353 (1939).
6. R. M. Fano: Jour. Frank. Inst. 249, 189-205 (1950); Technical Report No. 62, Research Laboratory of Electronics, M.I.T. (1948).
7. R. M. Fano: Jour. Frank. Inst., 249, 4, 139-147; Appendix II, 149-151 (1950); Technical Report No. 41, Research Laboratory of Electronics, M.I.T. (1948).
8. R. M. Fano: Loc. cit., Appendix I.
9. H. W. Bode: Network Analysis and Feedback Amplifier Design, Chap. XVII (Van Nostrand, N.Y. 1945).
10. G. E. Valley, Jr., H. Wallman: Loc. cit., Sec. 4.4.